observation of hysteresis are so long, however, that on a time scale of many days, the system is effectively bistable.

Acknowledgment. This work was supported by the National Science Foundation (Grants CHE 8419949 and CHE 8800169) and by a National Institutes of Health Postdoctoral Fellowship (Grant GM 10543) to W.P.H. We thank Robert Olsen, Johannes Reiter, John Rinzel, and Toby Sommer for helpful discussions.

Registry No. D, 7782-39-0.

A Transient Infrared Spectroscopy Study of Coordinatively Unsaturated Ruthenium Carbonyls

Paula L. Bogdan and Eric Weitz*

Contribution from the Department of Chemistry, Northwestern University, Evanston, Illinois 60208. *Received October 24, 1988*

Abstract: Transient infrared spectroscopy is used to study coordinatively unsaturated $Ru(CO)_x$ products formed by excimer laser photolysis of gas-phase $Ru(CO)_5$. Both $Ru(CO)_4$ and $Ru(CO)_3$ are photoproducts of 248- and 351-nm irradiation of $Ru(CO)_5$. This is the first report of direct observation of unsaturated $Ru(CO)_x$ species. Unlike the well-known $Fe(CO)_4$ fragment, the high reactivity of the $Ru(CO)_x$ species has precluded their observation in cryogenic studies. The rate constants for reaction of $Ru(CO)_4$ and $Ru(CO)_3$ with CO are $(2.8 \pm 0.8) \times 10^{-11}$ and $(7.6 \pm 0.3) \times 10^{-11}$ cm^3 molec^{-1} s^{-1}, respectively. These rate constants are $\sim 10^3$ greater than that for the reaction of $Fe(CO)_4$ with CO and can be rationalized in terms of the spin states of the reactants and products. Formation of a dinuclear complex, $Ru_2(CO)_9$, is also observed. Comparison of the distribution of $M(CO)_x$ fragments at different UV photolysis wavelengths has implications for the relative bond dissociation energies for carbonyl ligands on a ruthenium versus an iron center.

I. Introduction

Metal carbonyls are an important class of inorganic compounds. They can be used to thermally and/or photolytically produce reactive species that can induce homogeneous stoichiometric and catalytic transformations of organic substrates. They are also used as precursors to supported metal aggregates, thin films, and other solid-state materials. The dominant photochemical process for metal carbonyls is ligand dissociation, which provides open, highly reactive, coordination sites at the metal center. Details of the nature of these unsaturated species were first probed with matrix isolation techniques.[1] More recently, transient infrared spectroscopic studies of gas-phase unsaturated metal carbonyl photofragments have provided detailed information about the structure and reaction kinetics of these highly reactive species.[2]

One of the most well-studied of the metal carbonyls is $Fe(CO)_5$; its photofragments exhibit unique properties compared to those of other metal carbonyl compounds.[3,4] While $Fe(CO)_5$ has a singlet ground state, the unsaturated species $Fe(CO)_2$, $Fe(CO)_3$, and $Fe(CO)_4$ have been characterized as possessing triplet electronic ground states.[5] As a result, recombination of $Fe(CO)_4$ and CO to regenerate the singlet parent $Fe(CO)_5$ is comparatively slow. The gas-phase lifetime of $Fe(CO)_4$ in the presence of 100 Torr of CO is a relatively long 0.1 ms. This is in sharp contrast to the group 5 and 6 carbonyls, $V(CO)_6$, $Cr(CO)_6$, and $W(CO)_6$, whose ligand addition reactions take place on a potential energy surface of the same spin multiplicity. In these systems, photofragments have lifetimes on the order of microseconds with only 1 Torr of CO present.[6-8]

Another difference between $Fe(CO)_5$ and the group 6 carbonyls is that, upon 351-nm photolysis, $Fe(CO)_5$ loses two CO ligands while $Cr(CO)_6$ and $W(CO)_6$ give primarily $M(CO)_5$ photofragments. As a result of other studies it has been suggested that the $Fe(CO)_3$-CO bond is anomalously weak.[9] These results are compatible with this suggestion.

Since the electronic properties and product distribution of $Fe(CO)_5$ photofragments are unusual, it is of interest to speculate whether these are peculiar to iron itself or whether they prevail in the group 8 triad. The $M(CO)_5$ homologous series is known; however, the chemistry of $Ru(CO)_5$ and $Os(CO)_5$ has received far less attention than that of $Fe(CO)_5$. A major factor is the instability of the pentacarbonyls of osmium and ruthenium with respect to formation of the well-known $M_3(CO)_{12}$ species. In general, the stability of metal cluster species increases as one descends group 8 owing to an increase in M-M bond strength. Calculations have suggested that, unlike $Fe(CO)_4$, the $Ru(CO)_4$ fragment has a singlet electronic ground state.[10] We have chosen to study the gas-phase photochemistry of $Ru(CO)_5$, to compare and contrast the nature and reactivity of its photofragments with those of $Fe(CO)_5$.

Time-resolved infrared spectroscopy is used to determine the identities of unsaturated fragments following XeF and KrF excimer laser photolysis of $Ru(CO)_5$ and to determine microscopic rate constants for the reaction of these species with CO. Reactions of coordinatively unsaturated ruthenium species with $Ru(CO)_5$ have been observed and are discussed. Based on product distributions as a function of photolysis wavelength, comparisons of relative M-CO bond dissociation energies for iron and ruthenium can be made.

II. Experimental Section

The apparatus used in this study has been previously described.[11-14] Since it is both expensive and inconvenient to prepare and handle the amount of $Ru(CO)_5$ that would be needed for a flow cell, a change in

(1) Hitam, R. B.; Mahmoud, K. A.; Rest, A. J. *Coord. Chem. Rev.* **1984**, *55*, 1.
(2) Weitz, E. *J. Phys. Chem.* **1987**, *91*, 3945.
(3) Poliakoff, M.; Weitz, E. *Acc. Chem. Res.* **1987**, *20*, 408.
(4) Seder, T. A.; Ouderkirk, A. J.; Weitz, E. *J. Chem. Phys.* **1986**, *85*, 1977.
(5) Barton, T. J.; Grinter, R.; Thomson, A. J.; Davies, B.; Poliakoff, M. *J. Chem. Soc., Chem. Commun.* **1977**, 841.
(6) Ishikawa, Y.; Hackett, P. A.; Rayner, D. M. *J. Am. Chem. Soc.* **1987**, *109*, 6644.
(7) Seder, T. A.; Church, S. P.; Weitz, E. *J. Am. Chem. Soc.* **1986**, *108*, 4721.
(8) Ishikawa, Y.; Hackett, P. A.; Rayner, D. M. *Chem. Phys. Lett.* **1988**, *145*, 429.
(9) Engelking, P. C.; Lineberger, W. C. *J. Am. Chem. Soc.* **1979**, *101*, 5570.
(10) Ziegler, T. *Inorg. Chem.* **1986**, *25*, 2721.
(11) Ouderkirk, A. J.; Weitz, E. *J. Chem. Phys.* **1983**, *79*, 1089.
(12) Ouderkirk, A. J.; Wermer, P.; Schultz, N. L.; Weitz, E. *J. Am. Chem. Soc.* **1983**, *105*, 3354.
(13) Ouderkirk, A. J.; Seder, T. A.; Weitz, E. *SPIE Symp. Appl. Lasers Ind. Chem.* **1984**, *458*, 148.
(14) Seder, T. A.; Church, S. P.; Weitz, E. *J. Am. Chem. Soc.* **1985**, *107*, 1432.

0002-7863/89/1511-3163$01.50/0

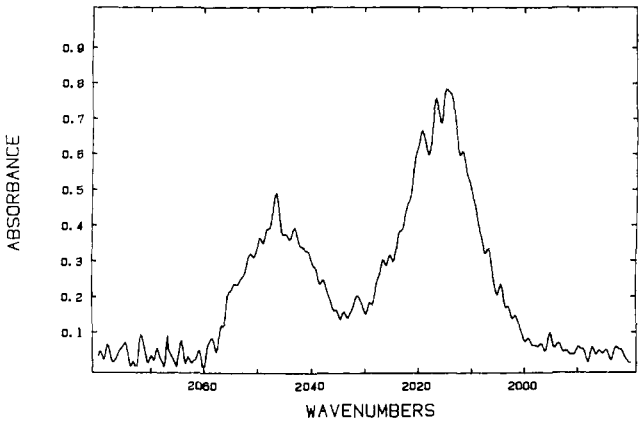

Figure 1. Gas-phase FTIR spectrum of $Ru(CO)_5$ taken at 20 ± 1 °C.

procedure versus previous studies is the use of static cell fills for the experimental measurements rather than a flow cell. Sample gases are introduced into a 16-cm gas cell with 2.4-cm diameter CaF_2 windows through a Teflon stopcock. Ruthenium pentacarbonyl is kept at −196 °C between cell fills. In the absence of CO, ruthenium pentacarbonyl is very unstable with respect to the formation of polynuclear ruthenium compounds. The workable lifetime of each cell fill is increased by addition of 1 Torr of CO. For consistency, each fill is always subjected to the same number of UV laser pulses. After each set of measurements, the cell is evacuated and then recharged. However, it is still necessary to periodically remove $Ru_3(CO)_{12}$ deposits from the cell windows.

The output of a UV excimer laser (Questek) operating at both 248 nm (KrF) and 351 nm (XeF) is used to photolyze $Ru(CO)_5$. Formation of unsaturated ruthenium carbonyl photoproducts is detected by their attenuation of infrared radiation from a home-built, line-tunable, liquid-nitrogen-cooled CO laser. Infrared beam intensity is monitored with a fast (τ rise = 35 ns) InSb detector. The detector output (transient waveform) is amplified (Perry X100), digitized, signal averaged (Lecroy 9400), and sent to computers for storage and manipulation. Time-resolved infrared spectra of the transients are constructed from the waveforms acquired at probe frequencies within the carbonyl stretch region by joining together the amplitude of various waveforms at particular common delay times.

Typical pressures of $Ru(CO)_5$ in the cell were on the order of 10–30 mTorr for KrF laser photolysis and 100–200 mTorr for XeF photolysis. Pressures of at least 10 Torr of Ar were used to assure that recombination reactions were in the high-pressure limit for the third body.[11-14] The infrared signals from each cell fill were normalized by comparing the attenuation of the excimer laser beam as measured by a photodiode; a ratio of the magnitude of the photodiode signal acquired during photolysis to that acquired after the cell is evacuated is proportional to the amount of $Ru(CO)_5$ present. A simple measurement of pressure is insufficient to determine $Ru(CO)_5$ concentration in the cell since $Ru(CO)_5$ decomposes on the walls of the cell. Excimer laser energies at the cell were approximately 2–3 mJ/cm^2 for KrF and 1 mJ/cm^2 for XeF.

Kinetic information is obtained by probing the relevant regions of the time-resolved infrared spectrum while varying the concentration of added CO. Resulting waveforms are analyzed as single or multiple exponentials by a Provencher routine.[15]

Ruthenium pentacarbonyl was synthesized by photolysis of an isopentane solution of $Ru_3(CO)_{12}$ (concentration <1 mg/mL)[16] under 1 atm of CO.[17] The photolysis was most conveniently carried out with Pyrex-filtered sunlight, but 420-nm lamps were used on cloudy days. Reaction is judged complete on bleaching of the isopentane solution from yellow ($Ru_3(CO)_{12}$) to clear ($Ru(CO)_5$). Upon completion of the reaction, the reaction mixture is separated by trap-to-trap distillation on a vacuum system. Because of the extreme instability of $Ru(CO)_5$ in the absence of CO, the distillation is carried out in the dark and done as rapidly as is possible without compromising the quality of the separation. The $Ru(CO)_5$ is condensed in a trap held at −84 °C (ethyl acetate/liquid N_2), while the solvent is collected at −196 °C.[18] The neat $Ru(CO)_5$ is

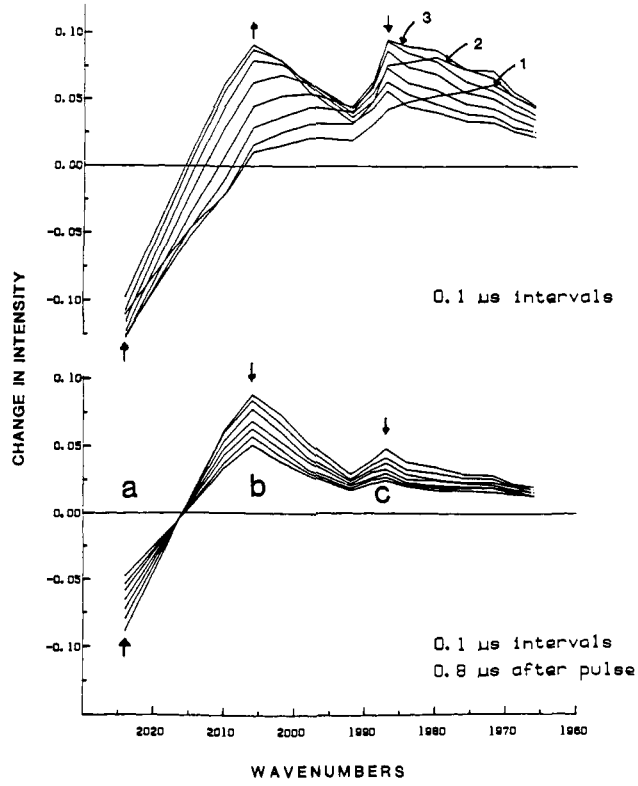

Figure 2. Transient time-resolved infrared spectra generated upon KrF laser photolysis of $Ru(CO)_5$. The top spectrum illustrates the evolution of the spectrum over the first 0.8-μs range, and the bottom spectrum shows the next 0.8-μs time period. See the text for assignments. Spectral traces are separated by 0.1-μs intervals and arrows indicate the direction of the peaks. The lower frequency peak in the top spectrum rises for the first three traces and then begins to decay.

Scheme I

$$Ru(CO)_5 \rightleftharpoons Ru(CO)_4 + CO$$

$$\downarrow \text{trimerization}$$

$$Ru_3(CO)_{12}$$

stored in the dark at dry ice temperatures under an atmosphere of CO. Even with these handling precautions, the effective yield of $Ru(CO)_5$ used in the experiments is only about 1% (based on $Ru_3(CO)_{12}$) as a result of adventitious decomposition. The isopentane solvent (Aldrich Gold Label) was dried over sodium and distilled before use. The gases used for the synthesis and experiments (CO and Ar) were obtained from Matheson and had stated purities of 99.995%.

III. Results and Discussion

By comparison with $Fe(CO)_5$, the structure of $Ru(CO)_5$ has been assigned, on the basis of its solution infrared spectrum, as trigonal bipyramidal.[19] Full force field calculations have been performed on data for isotopically labeled $Ru(CO)_5$ obtained in both solution and in liquid rare gases,[18] and have resulted in a complete assignment of the infrared spectrum. However, the gas-phase infrared spectrum has not been previously reported and is shown in Figure 1. The band at 2015 cm^{-1}, assigned as the e mode, involves stretches of the equatorial CO's; the higher frequency a_2 mode, at 2045 cm^{-1}, is associated with the axial CO stretches. The positions of these bands in hexane solution are 2002 and 2037 cm^{-1}, respectively.[20] In the absence of added CO, decomposition of the gas-phase $Ru(CO)_5$ is rapid. In a normal IR cell, the intensity of the infrared bands decreases by a factor of ~2 after 10 min.

(15) Provencher, S. W. *Biophys. J.* **1976**, *16*, 27; *J. Chem. Phys.* **1976**, *64*, 2772.
(16) Takats, J., personal communication. See also: Hastings, W. R.; Baird, M. C. *Inorg. Chem.* **1986**, *25*, 2913.
(17) Johnson, B. F. G.; Lewis, J.; Twigg, M. V. *J. Organomet. Chem.* **1974**, *67*, C75.
(18) Gregory, M. F.; Poliakoff, M.; Turner, J. J. *J. Mol. Struct.* **1985**, *127*, 247.
(19) Calderazzo, F.; L'Eplattenier, F. *Inorg. Chem.* **1967**, *6*, 1220.
(20) Rushman, P.; van Buren, G. N.; Shiralian, M.; Pomeroy, R. K. *Organometallics* **1983**, *2*, 693.

Scheme II

$$Ru(CO)_5 \xrightarrow{h\nu} Ru(CO)_x + (5-x)CO \quad \text{(i)}$$

$$Ru(CO)_x + CO \longrightarrow Ru(CO)_{x+1} \quad \text{(ii)}$$

$$Ru(CO)_x + Ru(CO)_5 \longrightarrow Ru_2(CO)_{5+x} \quad \text{(iii)}$$

$$x = 3, 4$$

Because of the propensity of $Ru(CO)_5$ to react with coordinatively unsaturated ruthenium carbonyls to form $Ru_3(CO)_{12}$, it is necessary to record the time-resolved infrared spectrum of gas-phase $Ru(CO)_5$ in the presence of added CO gas. As shown in Scheme I, $Ru(CO)_5$ has greater stability under these conditions. Reasonable signal-to-noise ratios are obtained for an average of 10 transients. The time-resolved spectrum obtained after KrF photolysis (248 nm) of $Ru(CO)_5$ is shown in Figure 2. The signals are recorded as differences in infrared radiation intensity relative to the CO laser intensity before UV laser photolysis. Changes in absorbance in the positive direction indicate an increase in the concentration of an absorbing species and changes in the negative direction correspond to depletion of an absorbing species.

Band Assignments. The spectrum in Figure 2 contains absorptions due to (at least) three different species. The highest frequency absorption, labeled a, is assigned to $Ru(CO)_5$. There is an initial depletion of $Ru(CO)_5$ on photolysis (Scheme II, eq i). Some $Ru(CO)_5$ is subsequently regenerated by reactions of its photoproducts with CO (Scheme II, eq ii). Reactions of $Ru(CO)_5$ with other species to form polynuclear products prevent total regeneration (Scheme II, eq iii). In Figure 2, peaks b and c are assigned to the unsaturated fragments $Ru(CO)_4$ and $Ru(CO)_3$, respectively. These assignments are based on several observations. First, in the $Fe(CO)_5$ system, owing to the change in degree of back-bonding on loss of CO, the positions of CO absorptions for the photoproducts shift to lower energy with an increase in coordinative unsaturation.[4] This trend is also expected for $Ru(CO)_5$ fragments. The second aid in assigning absorption bands concerns the relative degrees of internal excitation possessed by the $Ru(CO)_3$ and $Ru(CO)_4$ fragments. A KrF photon delivers more than enough energy to break two M–CO bonds; therefore, the photofragments that have lost only one CO on photolysis will be more internally excited than those that have lost two CO ligands.[2] As internally excited molecules are deactivated by collisions, their absorption bands narrow and shift to higher energy.[2] More internal excitation and a more dramatic shift to higher energy with time are observed for the band labeled b in Figure 2 relative to c. Band b is then compatible with an $Ru(CO)_4$ absorption. Finally, after the excited photoproducts have relaxed, an isosbestic point relates absorption b to a, which is assigned to $Ru(CO)_5$. An identification of the kinetic process involved in producing the isosbestic point as $Ru(CO)_4 + CO \rightarrow Ru(CO)_5$ is consistent with the other observations. Thus band b is assigned to $Ru(CO)_4$.

Since individual transients at 2000 cm^{-1} and higher energies show contributions from both $Ru(CO)_4$ and $Ru(CO)_5$ absorptions, it is unlikely that the true absorption maximum of $Ru(CO)_4$ is actually located at the peak of b (1998 cm^{-1}). It almost certainly lies to higher energy where it overlaps significantly with $Ru(CO)_5$ absorptions. This overlap has the effect of "pulling down" the $Ru(CO)_4$ absorption and making it appear to have an absorption maximum at lower frequency.

Because c is shifted to lower energy and shows less vibrational excitation than b by having a faster rise rate and smaller shift to higher frequency, c is assigned to $Ru(CO)_3$. This species is also present on XeF photolysis where ~80 kcal/mol is supplied by the incident photon. It would be very surprising if, in light of the expected bond dissociation energies of the $Ru(CO)_4$ species, which are discussed below, enough energy were available to produce significant quantities of $Ru(CO)_2$. This is especially true since, as will be discussed below, more energy appears to be required to produce $Ru(CO)_2$ than $Fe(CO)_2$, and *no* $Fe(CO)_2$ is observed on XeF photolysis of $Fe(CO)_5$. At even lower energy, the spectrum exhibits small positive absorptions out to 1909 cm^{-1}. These may be due to a tail of the $Ru(CO)_3$ absorption band or could also be due to small quantities of a species such as $Ru(CO)_2$. The absorptions in this region are insignificant compared to the rest of the spectrum. Thus, they have not been assigned.

Neither $Ru(CO)_3$ nor $Ru(CO)_4$ has previously been identified in solution or matrix/rare gas studies, though the $Ru(CO)_4$ intermediate is inferred from solution-phase kinetic studies of thermal ligand substitution in $Ru(CO)_5$.[23] A species that has been observed in matrix/liquid rare gas photolyses is $Ru_2(CO)_9$.[18] This relatively unstable compound had been previously synthesized[24] and decomposes to $Ru_3(CO)_{12}$ in a manner similar to $Ru(CO)_5$. In our study, there are absorptions in the regions 2050–2028, 2014–2006, and 1998 cm^{-1} that grow in a few microseconds after KrF photolysis of $Ru(CO)_5$. Since these absorptions are convoluted with those of other species, it is not possible to determine the actual number of IR bands that they represent. These transient signals remain above the difference spectral baseline after the disappearance of $Ru(CO)_4$ and $Ru(CO)_3$. The peaks reported for $Ru_2(CO)_9$ are at 2077, 2018, and 1814 cm^{-1} in low-temperature heptane solution.[24] From studies in liquid xenon, it has been speculated that there are other absorptions for $Ru_2(CO)_9$ that lie under those of the parent $Ru(CO)_5$ at 2002 cm^{-1}.[18] The absorption band around 2050–2028 cm^{-1} in the gas phase could correspond to the 2018-cm^{-1} solution band. The expected gas-phase positions of the 2077- and 1814-cm^{-1} solution bands have not been probed in our experiment. As would be expected, the magnitude of infrared absorptions suggested here as due to $Ru_2(CO)_9$ becomes smaller with decreased $Ru(CO)_5$ concentration. Further, the rate of appearance of the absorptions is not dependent on CO pressure, and is equal to the rate of disappearance of $Ru(CO)_4$. Therefore, the gas-phase absorptions at 2050–2028 cm^{-1} are likely due to $Ru_2(CO)_9$.

Bond Energies. Data from this and previous studies have implications for the relative bond dissociation energies from iron and ruthenium pentacarbonyls. Average M–CO bond dissociation energies are expected to be in the range of 25–43 kcal/mol.[21] Estimates based on thermodynamic data for the bond dissociation energies of one CO ligand from $M(CO)_5$ are 58 kcal/mol for Fe and 44 kcal/mol for Ru.[22] The substitution reactivity of $Fe(CO)_5$ versus $Ru(CO)_5$ in solution is consistent with a higher first CO dissociation energy from iron.[23] With XeF (351 nm) irradiation, the primary iron product is $Fe(CO)_3$, while in the case of $Ru(CO)_5$, both $Ru(CO)_3$ and $Ru(CO)_4$ are observed. Solution studies indicate that the $Fe(CO)_4$–CO bond is stronger than the $Ru(CO)_4$–CO bond, and assuming that, as expected, subsequent dissociation takes place on the ground electronic state potential energy surface,[2] it follows that the bond dissociation energy for loss of CO from $Ru(CO)_4$ is larger than that for CO loss from $Fe(CO)_4$. Thus, the bond dissociation energies for the first two CO's from $Ru(CO)_5$ appear to be similar and near to the average for metal carbonyls. This is unlike $Fe(CO)_5$, in which the $Fe(CO)_3$–CO bond is suggested as very weak.[9] With 248 nm photolysis, the predominance of $Ru(CO)_3$ and $Ru(CO)_4$ products from $Ru(CO)_5$ is in contrast with $Fe(CO)_5$, whose primary photoproduct is $Fe(CO)_2$. For $Fe(CO)_5$, the energy required to dissociate three CO ligands is estimated as approximately 95 kcal/mol.[9] Since little or no $Ru(CO)_2$ is observed with KrF photolysis, which delivers an energy of about 120 kcal/mol, and $Fe(CO)_2$ is observed with KrF photolysis of $Fe(CO)_5$, the average bond dissociation energy for loss of three CO ligands from ruthenium is likely greater than that for iron. These arguments are all based on the assumption of disposition of similar amounts of energy in the internal and translational degrees of freedom of the photofragments. Disposition of similar amounts of energy in internal degrees of freedom of the metal carbonyl and CO photofragment are consistent with experimental observations in the Fe[4] and Ru systems. Further, it is very unlikely that sufficiently large quantities of energy would be disposed in translational degrees of freedom of the photo-

(21) Connor, J. A. *Top. Current Chem.* **1977**, *71*, 71.
(22) Behrens, R. G. *J. Less-Common Met.* **1977**, *56*, 55.
(23) Huq, R.; Poë, A. J.; Chawla, S. *Inorg. Chim. Acta* **1980**, *38*, 121.
(24) Moss, J. R.; Graham, W. A. G. *J. Chem. Soc., Dalton Trans.* **1977**, 95.

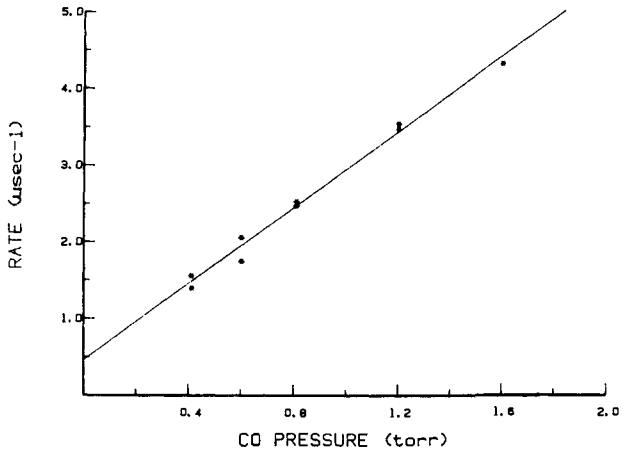

Figure 3. Plot of the pseudo-first-order rate constant for the reaction of $Ru(CO)_3$ with CO. The rate of disappearance of $Ru(CO)_3$ at 1975 cm^{-1} is plotted against the pressure of added CO. The slope of the line gives a bimolecular rate constant of $(7.6 \pm 0.3) \times 10^{-11}$ cm^3 $molec^{-1}$ s^{-1} for the $Ru(CO)_3 + CO \rightarrow Ru(CO)_4$ reaction.

fragments to affect our analysis.

Kinetics. The evolution of the time-resolved spectrum of $Ru(CO)_5$ with added CO can be described as an A → B → C system where A, B, and C are as follows:

$$\underset{A}{Ru(CO)_3} \xrightarrow[k_1]{CO} \underset{B}{Ru(CO)_4} \xrightarrow[k_2]{CO} \underset{C}{Ru(CO)_5} \qquad (1)$$

Since the CO concentration is in large excess compared to $Ru(CO)_x$, pseudo-first-order kinetics are expected and observed. The transient signals at a particular absorption wavelength are recorded at various CO pressures. The reaction rates are obtained by analyzing the signals as exponentials. The bimolecular rate constants k_1 and k_2 are then determined from the slope of the line resulting from the plots of reaction rate versus CO pressure. Extrapolation of the line for reaction rate versus CO pressure to $p(CO) = 0$ gives the rate for reaction of the $Ru(CO)_3$ or $Ru(CO)_4$ fragment with $Ru(CO)_5$.

The rates of reaction of $Ru(CO)_3$ with CO were determined by varying CO pressures and observing transients at 1957, 1975, and 1988 cm^{-1} after KrF photolysis. Transient signals were fit to an exponential rise and exponential fall where the fall is $k_1[CO]$. The data for 1975 cm^{-1} are shown in Figure 3. The slope of the least-squares line gives $k_1 = (7.6 \pm 0.3) \times 10^{-11}$ cm^3 $molec^{-1}$ s^{-1}. The data for transients at 1988 and 1957 cm^{-1} yield similar results. The intercepts, which give the rate of reaction of $Ru(CO)_3$ with $Ru(CO)_5$, are within experimental error of zero and indicate that the reaction of $Ru(CO)_3$ with parent does not compete effectively with CO addition at these pressures of CO and $Ru(CO)_5$. The bimolecular rate constant for reaction of $Fe(CO)_3$ with CO is $(2.2 \pm 0.3) \times 10^{-11}$ cm^3 $molec^{-1}$ s^{-1};[4] hence, both $Fe(CO)_3$ and $Ru(CO)_3$ recombine with CO with a rate constant that is within approximately an order of magnitude of the gas kinetic collision frequency of $\sim 5.0 \times 10^{-10}$ cm^3 $molec^{-1}$ s^{-1}.[25]

The determination of rates for the B → C process, eq 3, proved experimentally more difficult. Though the transient signals for $Ru(CO)_4$ following KrF irradiation of $Ru(CO)_5$ at 1998 and 2005 cm^{-1} have an exponential fall due to reaction with CO (eq 3), they

$$Ru(CO)_3 + CO \xrightarrow{k_1} Ru(CO)_4 \qquad (2)$$

$$Ru(CO)_4 + CO \xrightarrow{k_2} Ru(CO)_5 \qquad (3)$$

$$Ru(CO)_4 + Ru(CO)_5 \xrightarrow{k_3} Ru_2(CO)_9 \qquad (4)$$

do not exhibit a single exponential rise. The rise of the $Ru(CO)_4$ transient is determined by relaxation of nascent internally excited $Ru(CO)_4$ along with the appearance of $Ru(CO)_4$ from reaction of $Ru(CO)_3$ with CO (eq 2) and, in addition, is convoluted with the detector response time and possibly the appearance of $Ru_2(CO)_9$. In principle, the rate of reaction of $Ru(CO)_4$ can be measured by monitoring the reappearance of the $Ru(CO)_5$ absorption (eq 3). However, because of the overlap of an $Ru_2(CO)_9$ band with the 2019-cm^{-1} $Ru(CO)_5$ absorption, it is still difficult to obtain a good fit of the data at 2019 cm^{-1} to a single exponential rise and fall. Unfortunately, there are no other available $Ru(CO)_5$ absorbances that are free from overlap with those of some other species.

In an attempt to determine k_2 more accurately, XeF (351 nm) photolysis was employed. It was anticipated that $Ru(CO)_4$ would comprise more of the nascent photoproducts following XeF photolysis and would be formed with less internal energy than following KrF photolysis. However, because of the small UV absorption coefficient of $Ru(CO)_5$ at 351 nm, it was necessary to use up to 10 times the amount of $Ru(CO)_5$ parent per cell fill versus that used for KrF photolysis. Reaction 4 is then competitive with (3) under the typical CO pressures used (0.5 to 2 Torr). Competition from (4) could not be overcome by increasing the CO pressure, because the rate of (3) is sufficiently fast that a further increase in CO pressure greatly reduces the number of data points available for an exponential fit of the falling part of the signal. As a result there is still significant error in the determination of k_2 from monitoring $Ru(CO)_4$ following XeF photolysis.

Because of these difficulties, the bimolecular rate constant k_2 is known with less certainty than k_1. Values were determined using data for $Ru(CO)_4$ absorption at 2005 and 1998 cm^{-1} following KrF photolysis. The reaction rates for $Ru(CO)_4$ with CO were determined by fitting only the part of the transient corresponding to the decay of the $Ru(CO)_4$ absorption. We report the average value of the rate constant determined from these sets of data as $(2.8 \pm 0.8) \times 10^{-11}$ cm^3 $molec^{-1}$ s^{-1}. This bimolecular rate constant is of the same order as those for $Ru(CO)_3 + CO$ and $Fe(CO)_3 + CO$, $(7.6 \pm 0.3) \times 10^{-11}$ and $(2.2 \pm 0.3) \times 10^{-11}$ cm^3 $molec^{-1}$ s^{-1}, respectively. These rate constants are all approximately three orders of magnitude greater than the rate constant for reaction of $Fe(CO)_4 + CO$, $(5.8 \pm 1.5) \times 10^{-14}$ cm^3 $molec^{-1}$ s^{-1}.[4] Since $Fe(CO)_4$ is known to have a triplet electronic ground state and $Fe(CO)_5$ has a singlet ground-state configuration, the reaction to regenerate $Fe(CO)_5$ by reaction of $Fe(CO)_4$ with CO is spin-forbidden. The mononuclear iron photofragments $Fe(CO)_x$ ($x = 2, 3, 4$) are all believed to have triplet ground states,[4] so the final recombination to generate singlet $Fe(CO)_5$ is slower than the preceding CO recombination steps. In contrast, both $Ru(CO)_3$ and $Ru(CO)_4$ recombine quickly with CO. There is no evidence to indicate that the ground state of $Ru(CO)_5$ is other than the expected singlet configuration and, on the basis of Hartree–Fock–Slater calculations, the $Ru(CO)_4$ fragment has also been predicted to have a singlet electronic state.[10] The experimental results support the idea of a singlet ground state for the $Ru(CO)_x$ fragments. Furthermore, singlet states are expected to be lower in energy for second- and third-row metal compounds owing to lower spin-pairing energies.[10] However, heavy metal atoms can significantly increase rates of singlet–triplet interconversion.[26] Thus, the large rate constants for k_1 and k_2 are not conclusive proof that $Ru(CO)_3$ and $Ru(CO)_4$ have gound-state singlet configurations. Nevertheless, they are certainly suggestive of this conclusion.

Following XeF photolysis of $Ru(CO)_5$, the intercept for the plot of rate for reaction of $Ru(CO)_4$ versus CO pressure is significantly positive. This is due to reaction 4, which is CO pressure independent. The rate constant for (4) is approximately 10^{-9} cm^3 $molec^{-1}$ s^{-1}. The rate constant is consistent with rates obtained by analysis of the rise of the $Ru_2(CO)_9$ absorption from transients in the 2028–2050-cm^{-1} range. We report this rate constant as an order of magnitude number because of the difficulty of exactly determining the concentration of $Ru(CO)_5$ in our reaction cell

(25) This value is the calculated collision frequency for one molecule of $Ru(CO)_5$ with 1 Torr of CO in the IR cell at 20 °C.

(26) Steinfeld, J. I. *Molecules and Radiation*; Harper and Row: (1974).

due to its continuous decomposition. It should, of course, be realized that the exact concentration of $Ru(CO)_5$ is unimportant for determination of rate constants of CO addition reactions since these are run under pseudo-first-order conditions. As a comparison, the rate constant for formation of $Fe_2(CO)_8$ in the gas phase is of similar magnitude, $\sim 10^{-9}$ cm^3 molec^{-1} s^{-1}.[27] Rate constants for formation of dinuclear metal carbonyl species tend to be larger than those for the reaction of the monometallic photofragments with CO.

$Ru(CO)_4$ Geometry. The lowest energy geometry for $Ru(CO)_4$ is predicted as D_{2d}, with C_{2v} as the next most favorable.[10] The overlap of infrared bands makes determination of photofragment geometry a difficult problem. As both symmetries have two IR active modes, isotopic labeling would be necessary to determine the structure unambiguously. These experiments are beyond the scope of this report.

IV. Conclusions

Photolysis of gas-phase $Ru(CO)_5$ with UV (248 and 351 nm) radiation produces $Ru(CO)_3$ and $Ru(CO)_4$. These fragments recombine with CO with rate constants $(7.6 \pm 0.3) \times 10^{-11}$ and $(2.8 \pm 0.8) \times 10^{-11}$ cm^3 molec^{-1} s^{-1}, respectively, which are both within approximately an order of magnitude of the gas kinetic rate constant. In addition, $Ru(CO)_4$ reacts with parent to form $Ru_2(CO)_9$. The reactivity of $Ru(CO)_4$ is markedly different from $Fe(CO)_4$. Recombination of $Fe(CO)_4$ with CO occurs at a rate $\sim 10^3$ slower than the ruthenium analogue because the reaction of $Fe(CO)_4$ with CO is spin-forbidden. The photoproducts of $Ru(CO)_5$ at 248 nm are almost exclusively $Ru(CO)_3$ and $Ru(CO)_4$. More $Ru(CO)_4$ is formed with 351-nm irradiation, but significant amounts of $Ru(CO)_3$ are also observed. Since the predominant products in $Fe(CO)_5$ photolysis are $Fe(CO)_2$ at 248 nm and $Fe(CO)_3$ at 351 nm, the average bond dissociation energies for the loss of three CO ligands from ruthenium are expected to be greater than that for the corresponding Fe–CO bonds. The first and second bond dissociation energies for sequential CO loss from $Ru(CO)_5$ appear to be similar and close to average, whereas the first and second CO bond dissociation energies for $Fe(CO)_5$ are considered to be significantly higher and lower respectively than the average for M–CO bonds. The relative instability of $Ru(CO)_5$ versus $Fe(CO)_5$ toward decomposition to the $[M(CO)_4]_3$ species can be rationalized on this basis.

Acknowledgment. We thank the National Science Foundation for support of this work under NSF Grant No. CHE 88-06020, and we acknowledge support of the donors of the Petroleum Research Fund administered by the American Chemical Society under Grant No. 18303-AC6, 3-C. The experimental assistance of Steven Gravelle was greatly appreciated.

(27) Ryther, R.; Weitz, E., to be published.

Collision-Induced Dissociation of Niobium Cluster Ions: Transition Metal Cluster Binding Energies

S. K. Loh,[†] Li Lian,[‡] and P. B. Armentrout*[,‡,§]

Contribution from the Departments of Chemistry, University of California, Berkeley, California 94720, and the University of Utah, Salt Lake City, Utah 84112.
Received October 21, 1988

Abstract: The cross sections for collision-induced dissociation (CID) of Nb_n^+ (n = 2–6) with Xe are presented. Experiments are conducted on a recently constructed guided ion beam mass spectrometer, which produces intense beams of thermalized, mass-selected, niobium cluster ions. Nb_n^+ are observed to fission to all possible ionic fragments and the largest possible neutral fragments at collision energies <10 eV. Evidence is presented for loss of multiple Nb atoms from the cluster at energies higher than 10 eV. This fragmentation pattern differs markedly from that previously observed for small iron cluster ions. CID thresholds are used to derive $D°(Nb_{n-1}^+–Nb)$ for n = 2–6, along with $D°(Nb_m)$ and ionization potentials (IPs) of Nb_m for m = 2 and 3. By using known IPs, $D°(Nb_n)$ for n = 4, 5, and 6 are also obtained. Nb_2^+ is found to be the most strongly bound cluster ion, $D°(Nb^+–Nb) = 6.15 \pm 0.15$, and Nb_3^+ is the most weakly bound cluster ion, $D°(Nb_2^+–Nb) = 4.60 \pm 0.15$ eV.

I. Introduction

Metal clusters constitute a new and exciting regime of matter, affording the opportunity to study changes in metal chemistry as a function of the number of metal atoms. Studies of transition-metal clusters are potentially applicable to an understanding of catalysis and oxidation processes that occur on surfaces or surface imperfections. Such studies in the gas phase can be used to probe the reactivity of the bare cluster, in the absence of complicating solvent effects. More complex processes can then be simulated by ligating the cluster and carrying out analogous reactions. Within the last 10 years, technological developments have made gas-phase studies possible.[1] Now, the information needed to quantitatively characterize cluster chemistry is beginning to accumulate.

Bond dissociation energies (BDEs) of clusters are important pieces of information that have gone largely uncharacterized. These are quantities that are essential to an understanding of reaction thermochemistry, since many reactions involve metal–metal bond cleavage and formation of new bonds with the reactant molecule. Although quantitative BDE measurements have been made on all first-row and many second-row transition-metal dimers,[2] such experimental work on larger gas-phase main-group metal[3,4] and transition-metal[5,6] clusters is scarce. All previously

[†] University of California.
[‡] University of Utah.
[§] Author to whom correspondence should be addressed. NSF Presidential Young Investigator, 1984–1989; Alfred P. Sloan Fellow; Camille and Henry Dreyfus Teacher-Scholar, 1988–1993.

(1) Dietz, T. G.; Duncan, M. A.; Powers, D. E.; Smalley, R. E. *J. Chem. Phys.* **1981**, *74*, 6511. Bondybey, V. E.; English, J. H. *J. Chem. Phys.* **1982**, *76*, 2165.
(2) Morse, M. D. *Chem. Rev.* **1986**, *86*, 1049.
(3) See for examples: Hanley, L.; Anderson, S. L. *J. Phys. Chem.* **1987**, *91*, 5161. Ruatta, S. A.; Anderson, S. L. *J. Chem. Phys.* **1988**, *89*, 273.
(4) Jarrold, M. F.; Bower, J. E. *J. Chem. Phys.* **1987**, *87*, 1610. Jarrold, M. F.; Bower, J. E. *J. Am. Chem. Soc.* **1988**, *110*, 70.
(5) Brucat, P. J.; Zheng, L.-S.; Pettiette, C. L.; Yang, S.; Smalley, R. E. *J. Chem. Phys.* **1986**, *84*, 3078.
(6) Loh, S. K.; Lian, L.; Hales, D. A.; Armentrout, P. B. *J. Chem. Phys.* **1988**, *89*, 610.

0002-7863/89/1511-3167$01.50/0